Journal of Physics: Conference Series **160** (2009) 012004 doi:10.1088/1742-6596/160/1/012004

Performance and Operation of the *BABAR* Calorimeter

A. M. Ruland

Department of Physics, The University of Texas at Austin, 1 University Station C1600, Austin, Tx 78712-0264

E-mail: ruland@physics.utexas.edu

(For the BABAR calorimeter group)

Abstract. The performance and operation of the CsI(Tl) crystal calorimeter of the *BABAR* detector during the last years of operation is discussed.

1. Introduction

The *BABAR* detector is located at the PEP-II B Factory at the Stanford Linear Accelerator Center (SLAC). PEP-II is an asymmetric e^+e^--collider operating mainly at a center-of-mass energy of 10.58 GeV. This corresponds to the mass of the $\Upsilon(4S)$ resonance, which decays exclusively into $B^0\overline{B}^0$ and B^+B^- pairs. One main physics goal of the *BABAR* experiment was the measurement of CP-violating asymmetries in the decay of neutral B-mesons. Other goals of the experiment include precision measurements of the decays of bottom mesons to charm and τ leptons, as well as searches for rare decays utilizing the high luminosity delivered by the PEP-II accelerator. The *BABAR* detector (Fig 1) consists of 6 subdetectors. Starting from the interaction point and moving radially outwards there is a Silicon Vertex Detector, Drift Chamber, DRC (Cherenkov detector), an Electromagnetic Calorimeter, and an Instrumented Flux Return.

2. Calorimeter Goals

The calorimeter is designed for excellent efficiency, energy and angular resolutions over the energy range 20 MeV to 9 GeV. These requirements the choice for *BABAR* of a CsI(Tl) crystal calorimeter. The energy resolution of a homogeneous crystal calorimeter is given empirically as two terms summed in quadrature:

$$\frac{\sigma_E}{E} = \frac{a}{\sqrt[4]{E(\,\mathrm{GeV})}} \oplus b, \tag{1}$$

where E and σ_E refer to the energy of a photon and its' RMS error in GeV. The energy dependent term, a, arises from fluctuations in photon statistics, electronics noise, and beam background generated noise. The constant term, b, arises from non-uniformity in light collection, leakage or absorption in the material between and in front of the crystals, and uncertainties in the calibration. The angular resolution is determined from the transverse crystal size and distance

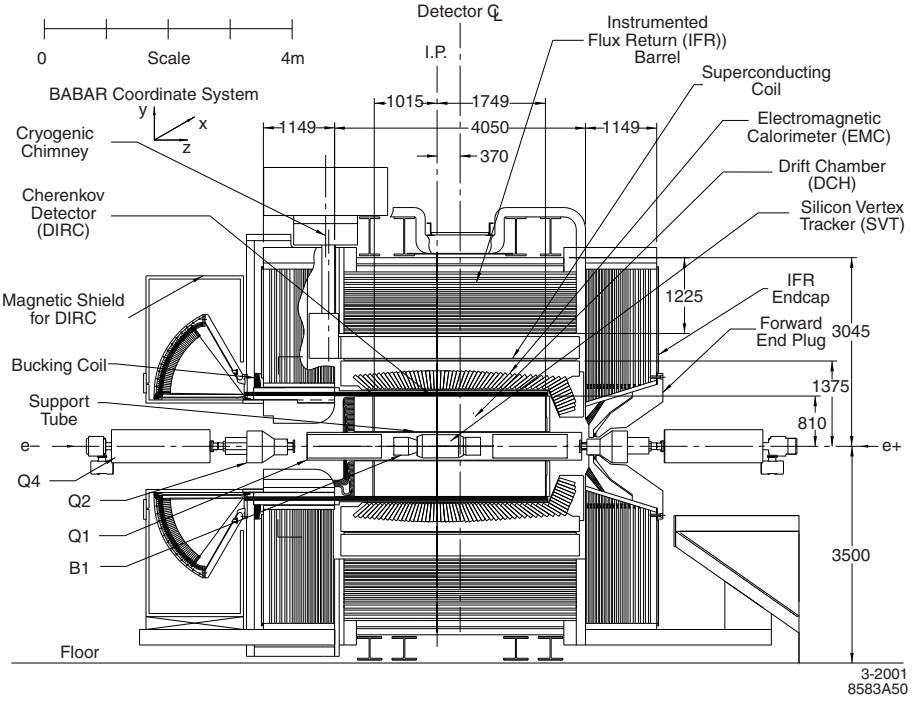

Figure 1. Longitudnal cross-section of the *BABAR* detector

from the interaction point. It can be empirically described by the equation

$$\sigma_\theta = \sigma_\phi = \frac{c}{\sqrt{E(\,\mathrm{GeV})}} + d, \tag{2}$$

3. Calorimeter Layout and Assembly

The *BABAR* calorimeter consists of 6580 CsI(Tl) crystals. The angular coverage is 126° in polar angle and 360° in azimuthal angle corresponding to a solid angle coverage of 90° in the center-of-mass (Fig 2). It is divided into two mechanically distinct sections: a barrel (5760 crystals) and an endcap (820 crystals). The barrel is subdivided into 48 polar angle rings with 120 crystals per ring. The endcap consists of 8 polar angle rings with the inner two rings containing 80 crystals each, the next 3 rings contain 100 crystals each, while the outermost 3 rings contain 120 crystals each. The geometry of the calorimeter is projective in ϕ, while in θ there is a non-projectivity of 14 mrad, except in the transition region between the barrel and endcap where it reaches 45 mrad. This non-projectivity minimizes energy losses through the spaces between the crystals. The 2 mm gap between the barrel and endcap is fully covered by the non-projectivity.

3.1. Crystal Assembly

The crystals are grown from CsI doped with 0.1% Thallium. They are trapezoidal in shape with a typical front(rear) dimensions of $4.7 \times 4.7(6.1 \times 6.0)$ cm^2. The length of the crystals varies from 16 radiation lengths, X_0, in the backward part of the barrel to 17.5 X_0 in the forward part. For the details on the complete fabrication and assembly of the crystals see [1].

3.2. Mechanical Assembly

The individual crystals are assembled in carbon fiber modules. In the barrel, the modules contain 7×3 crystals in $\theta \times \phi$, except for the backward most module which contains 6×3

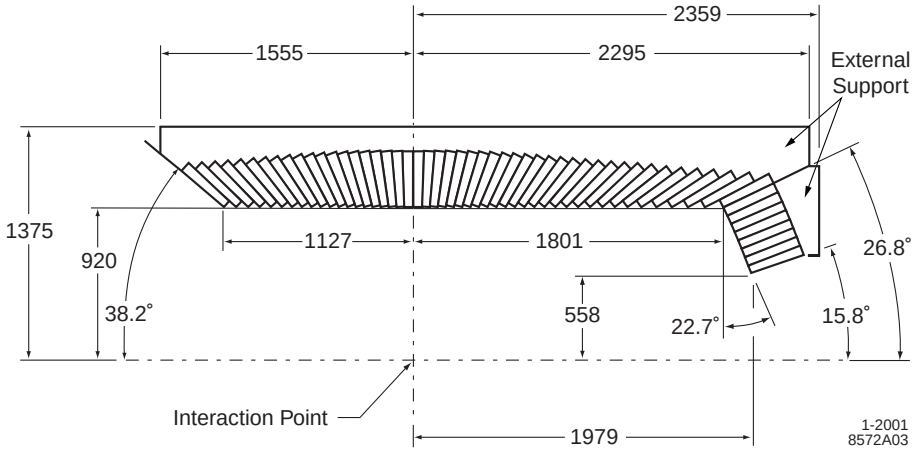

Figure 2. Longitudinal cross-section of the Calorimeter. Dimensions in mm.

crystals. The barrel consists of 280 modules which are inserted into an aluminum cylinder. The endcap contains 20 identical modules each with 41 crystals which are bolted to one of two semi-circular support structures.

4. Performance

4.1. π^0 and η mass and width

Fig 3a shows that two-photon invariant mass for hadronic events around the π^0 mass in data from 2001. Photons are required to exceed 30 MeV, while the π^0 energy is required to exceed 300 MeV. The reconstructed mass is measure to be 134.9 MeV/c^2, with a width of 6.5 MeV/c^2. The two-photon invariant mass for symmetric η's for $E_\eta > 1$ GeV is shown in Fig 3b. The reconstructed mass is 547 MeV/c^2, with a width if 15.5 MeV/c^2.

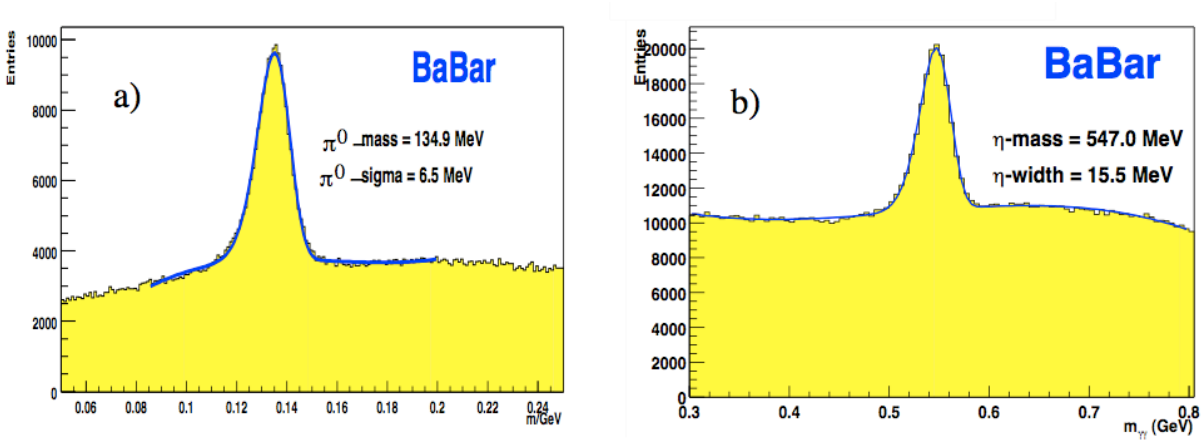

Figure 3. Invariant mass of the photons in hadronic events for π^0 mass (a) and η mass (b). The solid lines are fits to the data.

4.2. Resolution

Fig 4 shows the energy and angular resolution of the calorimeter derived from a variety of processes: radioactive source, symmetric π^0 and η decays, $\chi_{c1} \rightarrow J/\psi\gamma$, and Bhabha events. As the energy resolution of the π^0 and η is dependent on the calorimeter angular resolution, a simultaneous fit to energy and angular resolution was done for those cases, assuming an asymmetry of the photon energy distribution derived from Monte Carlo. A smearing of the MC energies is applied in order to have good agreement between Data and MC. The data from the radioactive source calibration shows a deviation form the fitted curve, as the photons from this process develop in single crystals and do not traverse material in front of the calorimeter. The angular resolution (Fig 4b) is derived from symmetric π^0 and η decays. Fits to the data yield

$$\frac{\sigma_E}{E} = \frac{(2.30 \pm 0.03 \pm 0.3)\%}{\sqrt[4]{E(\,\mathrm{GeV})}} \oplus (1.35 \pm 0.08 \pm 0.2)\%, \tag{3}$$

$$\sigma_\theta = \sigma_\phi = \frac{(4.16 \pm 0.04)\mathrm{mrad}}{\sqrt{E(\,\mathrm{GeV})}} + (0.0 \pm 0.0)\mathrm{mrad}. \tag{4}$$

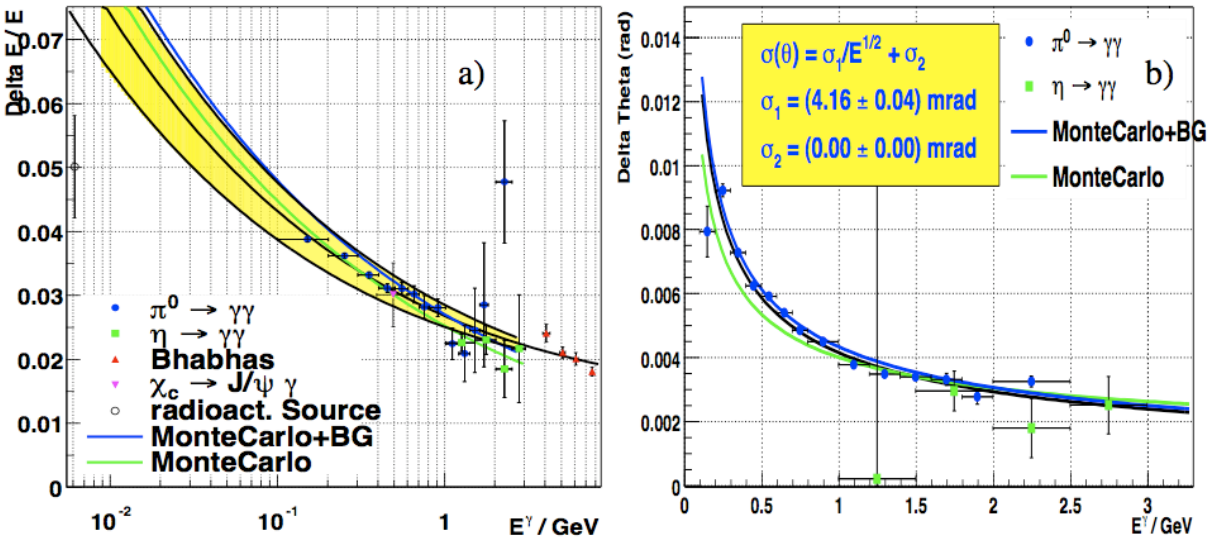

Figure 4. Energy resolution (a) and angular resolution (b). The central black line is a fit to the data. The outer black lines in (a) show the systematic uncertainty.

5. Calibrations

In spite of careful selection and tuning of the crystals, their light yield varies significantly and is non-uniform along the crystal axis. The light yield also changes over time due to backgrounds from beam-generated radiation. These differences in light yield must be calibrated away at different energies, corresponding to different average shower penetration. The calibration of the deposited energies is performed at two energies at the opposite ends of the dynamic range. The measurements are then combined by a logarithmic interpolation. At the low end of the range a 6.13 MeV photon from a radioactive source provides an absolute calibration, while at higher energies the relation between polar angle and energies of Bhabha events is used.

Corrections due to energy loss from shower leakage and absorption are performed as a function of polar angle and energy. For these corrections photons from π^0 decays are used with energies

from 70 MeV to 2 GeV and photons from $e^+e^- \to \mu^+\mu^-\gamma$ are used with energies 400 MeV to 6 GeV. The details of this shower correction are given in these proceedings [2].

5.1. Radioactive Source Calibration

The radioactive source calibration uses 6.13 MeV photons produced in the reaction

$$^{19}F + n \to ^{16}N + \alpha, ^{16}N \to ^{16}O^* + \beta, ^{16}O^* \to ^{16}O + \gamma. \quad (5)$$

A fluid of polychlorotrifluoro-ethylene, activated by neutrons from a generator, circulates through a system of tubes in front of the crystals. ^{16}N has a lifetime of 7 seconds. All crystals on the calorimeter are calibrated with this method. The average resolution is 0.33%. Fig 5a shows the relative light yield change of the crystals in different calorimeter regions as function of the delivered integrated luminosity. This calibration is performed every 4 ± 1 weeks.

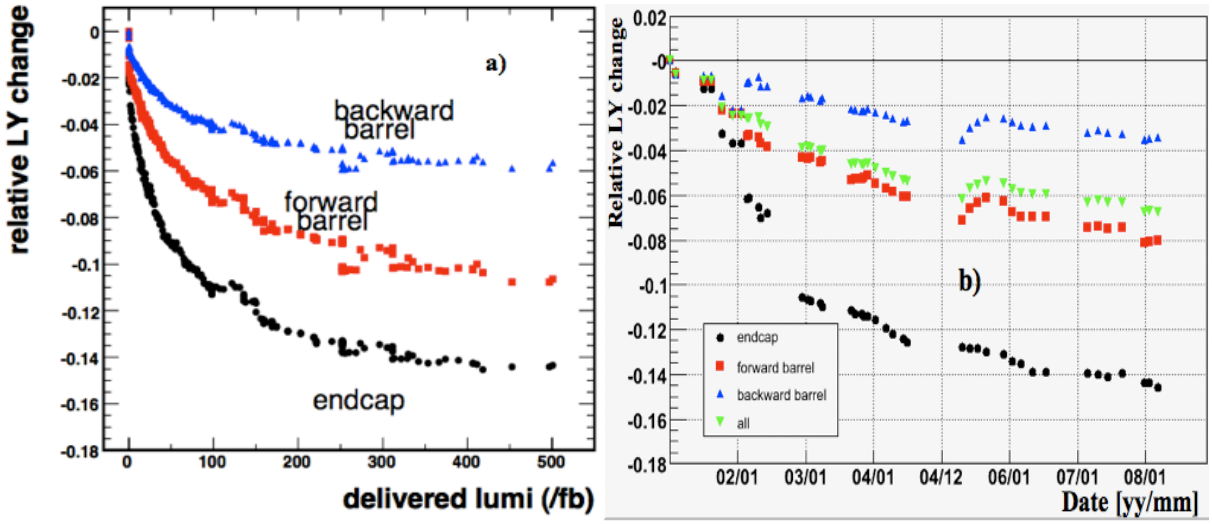

Figure 5. The relative light yield change for the radioactive source constants as a function of delivered luminosity (a) and the relative light yield change for Bhabha constants as a function of time (b).

5.2. Bhabha Calibration

At high energies, single crystal calibration is performed with a pure sample of Bhabha events. As a function of the polar angle of the $e^{\pm}$, the deposited cluster energy is constrained to equal that of a GEANT based Monte Carlo simulation. For a large number of energy clusters, a set of simultaneous linear equations relates the measured to the expected energy and thus permits the determination of a constant for each crystal. 200 $e^{\pm}$ hits per crystal result in constants with a statistical error of 0.35%. This calibration is done $\sim$1 per month. Fig 5b shows the relative change in light yield of the crystals as a function of time for 3 different regions of the calorimeter as well as for the full set of constants.

6. Diagnostics and Monitoring

Real-time monitoring of the calorimeter hardware, currents, voltages, and temperatures is done using the EPICS software package [3]. EPICS is a set of open source software tools, libraries, and applications for real-time monitoring of large scientific experiments.

Monitoring of the data is done in two separate passes. Initially, individual crystal parameters such as occupancies, hit timing, and multiplicity are extracted from the data as it is recorded. Automatic notification to the shifters is given when a parameter goes outside of preset boundaries. Secondly, fully reconstructed events are available within hours and provide higher level benchmarks such as π^0 mass and width, energy-momentum ratios, and track-cluster matching efficiencies.

6.1. Lighpulser Monitoring

Daily monitoring of the readout path from the crystals diodes to the DAQ system is performed using a lightpulser system. Spectrally filtered light is transmitted from a Xenon lamp to the rear of each crystal. The light pulse is similar in characteristics to scintillation light from CsI(Tl) crystals over the range of all but the lowest deliverable energies. This system allows for early detection of electronics issues that would affect data taking, as well as for monitoring relative lightyield changes in crystal response on a short time scale between calibrations.

6.2. Radiation Monitoring

Beam generated backgrounds are the major cause of reduction in the light yield of the crystals over time. In order to monitor this source of background, 116 RadFETs are placed in front of the calorimeter barrel and endcap crystals. These RadFETs are real-time integrating dosimeters based on solid-state MOS technology and are integrated into the EPICS monitoring system. As can be seen by Fig 6, the integrated dose is largest in the endcap which is closer the the beam line as well as more forward in polar angle making it more susceptible to beam generated background photons from small angle radiative Bhabha events in which an $e^{\pm}$ strikes a machine element.

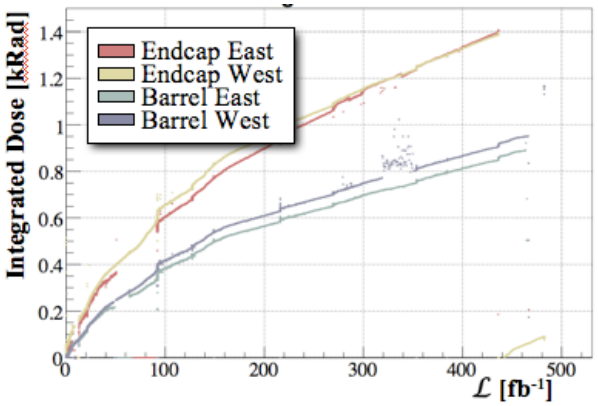

Figure 6. Average integrated dose for the barrel and endcap subdivided into east and west sides as a function of delivered luminosity.

7. Summary

The *BABAR* experiment concluded data taking in April 2008. For the past several years the Electromagnetic Calorimeter was recording data with high efficiency and excellent quality.

References

[1] *BABAR* Collaboration 2002 *Nucl. Inst. Meth.* **A479** 1.
[2] J.Marks, in these Proceedings.
[3] http://www.aps.anl.gov/epics/.